Int. J. Solids Structures Vol. 30, No. 21, pp. 2937–2951, 1993
Printed in Great Britain

0020–7683/93 $6.00+ .00

DYNAMIC CRACK GROWTH ALONG ELASTIC–PLASTIC INTERFACES

XIAOMIN DENG
Department of Mechanical Engineering, University of South Carolina, Columbia, SC 29208, U.S.A.

(Received 7 December 1992)

Abstract—Asymptotic, plane strain near-tip fields are presented for steadily propagating interface cracks between (1) a ductile solid and a rigid substrate, and (2) two dissimilar ductile solids. The ductile materials are taken to be incompressible, elastic–perfectly plastic and obey the J_2-flow theory of plasticity. It is shown that the crack-tip region can be considered as being composed of two types of angular plastic sectors: Uniform sectors, in which stresses are constant, and nonuniform sectors. Solutions for the asymptotic crack-tip fields are not unique, and they are represented by various assemblies of the plastic sectors that satisfy the necessary conditions. Some of the solutions are isolated, while others belong to one-parameter families. The crack-tip fields represented by these asymptotic solutions are fully continuous in each of the two component solids, and have nonsingular strains at the crack tip.

INTRODUCTION

The asymptotic structure of the elastic–plastic crack-tip fields around an interfacial crack in a dissimilar bimaterial has been the focus of many recent investigations. For stationary interface cracks, such investigations were led by finite element studies of cracks in power-law hardening materials under small-scale yielding conditions (Shih and Asaro, 1988, 1989), revealing distinct as well as similar features when compared to mixed-mode crack-tip fields in homogeneous materials, which prompted several investigators to conduct further research on this subject using analytical means (Guo and Keer, 1990a; Gao and Lou, 1990; Wang, 1990; Champion and Atkinson, 1990, 1991). In the case of interface cracks in elastic–perfectly plastic materials, analytic asymptotic solutions were obtained by Guo and Keer (1990b) and Deng (1992), and numerical small-scale yielding solutions by Zywicz and Parks (1992). For cracks with frictionless crack-surface contact, analyses have been performed by Zywicz and Parks (1990), Aravas and Sharma (1991), and Sharma and Aravas (1991).

In the area of interfacial crack growth, the investigation of asymptotic structures of the near-tip elastic–plastic fields was pioneered by Guo and Keer (1990b), who obtained an asymptotic field solution for a plane strain crack growing steadily and quasi-statically along an interface between an elastic–perfectly plastic solid and a rigid substrate. This and similar problems were later investigated independently by several other authors. Ponte Castaneda and Mataga (1991) treated the same problem and found two asymptotic near-tip field solutions, one of which coincides with that of Guo and Keer. Ponte Castaneda and Mataga further obtained steady-state, asymptotic and variable-separable solutions for quasi-statically growing cracks along ductile/brittle interfaces under both plane strain and anti-plane strain conditions, where the ductile solid is elastic–plastic with linear hardening and the brittle solid is linearly elastic. Drugan (1991) studied the problem of steady, quasi-static crack growth along the interface between an elastic–perfectly plastic solid and a rigid substrate under plane strain as well as anti-plane strain conditions. By admitting proper velocity discontinuities, Drugan found two families of asymptotic near-tip solutions for the plane strain case and one family for the anti-plane strain case. It is noted that the plane strain solutions for the ideally-plastic/rigid interface by Guo and Keer, and Ponte Castaneda and Mataga are contained in Drugan's families of solutions.

The study reported in this paper extends the above elastic–plastic analyses of quasi-static, interfacial crack growth to the dynamic case, which takes into consideration the effects of inertia on the crack-tip fields. Besides its theoretical relevance, this problem also has practical bearings, in that crack growth along an inherently weak bond between two dissimilar materials will probably be trapped in the interface, and under certain conditions may become unstable and start to propagate rapidly along the interface. Since this is a first-order asymptotic analysis, the condition of steady-state crack growth is assumed, as is done in previous studies for the case of quasi-static crack growth. The two component materials are treated as either rigid or elastic–plastic (ductile), which, in the latter case, are elastic–perfectly plastic, incompressible, and obey the J_2-flow theory of plasticity. In the following, a concise formulation of the mathematical problem will be presented first, with solutions for each crack-tip sector given explicitly. Then the sectors will be assembled for both ductile/rigid and ductile/ductile interfaces, and several one-parameter families of solutions, as well as some isolated ones, of the crack-tip fields will be obtained. Finally we will study the solutions, discuss their features and summarize the main findings of this study.

FORMULATION

As shown in Fig. 1, we consider a straight crack growing steadily yet dynamically along the interface between two dissimilar materials, where the (moving) coordinate system is originated at the crack tip, with x_1 and x_2 as indicated, and x_3 normal to the plane pointing outwards, and r and θ are the associated polar coordinates. The upper material is elastic–plastic (ductile) and the lower one is either rigid (nondeformable) or ductile. (We note that when a ductile material is in a purely elastic state, it is equivalent to an elastic material.) The governing equations given below will be for a generic ductile solid, and can apply to either of the two component materials in question.

Now let σ_{ij} be the rectangular Cartesian components of the stress tensor, and similarly, ε_{ij} the components of the strain tensor, and v_i the components of the velocity vector, where Latin indices have the range 1, 2 and 3, and later, Greek indices will have the range 1 and 2. If we note that the steady-state condition requires that the crack speed v be a constant and that $(\dot{\ }) = -v(\ )_{,1}$, where a superimposed dot denotes a material time derivative and a comma implies spatial derivatives with respect to coordinate components following it, the equation of motion, with inertia included, can be written as

$$\sigma_{\alpha\beta,\beta} = -\rho v v_\alpha. \tag{1}$$

The relation between the components of the (small) strain-rate tensor and the velocity vector is

$$\dot{\varepsilon}_{\alpha\beta} = (v_{\alpha,\beta} + v_{\beta,\alpha})/2. \tag{2}$$

The constitutive law for the generic incompressible elastic–perfectly plastic material is given by

$$\dot{\varepsilon}_{\alpha\beta} = (1/2\mu)\dot{s}_{\alpha\beta} + \lambda s_{\alpha\beta}, \tag{3}$$

where μ is the elastic shear modulus. The flow factor λ is non-negative in a plastic state and

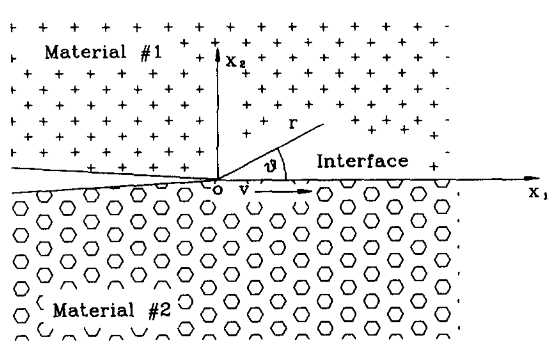

Fig. 1. A straight crack propagating dynamically along a bimaterial interface.

identically zero in an elastic state, and $s_{ij} = \sigma_{ij} - \sigma\delta_{ij}$ is the component of the deviatoric stress tensor, where $\sigma = \sigma_{kk}/3$ (the summation convention associated with indicial notations is adopted here) is the mean or hydrostatic stress and δ_{ij} is the Kronecker delta. Due to the plane strain requirement $v_3 = \varepsilon_{3i} = \sigma_{3\beta} = 0$ and the incompressibility of the material, we find that

$$v_{\alpha,\alpha} = 0, \quad \sigma = \sigma_{\alpha\alpha}/2 = \sigma_{33}, \quad s_{11} = -s_{22} = (\sigma_{11} - \sigma_{22})/2, \quad s_{33} = 0, \tag{4}$$

from which the von Mises yield condition can be simply written as

$$s_{22}^2 + s_{12}^2 = k^2 \tag{5}$$

where constant k is the material's yield stress in pure shear.

To complete the mathematical formulation of the problem, we note that the above governing equations are supplemented by traction and velocity continuity conditions across the interface and the traction-free boundary conditions $\sigma_{12} = \sigma_{22} = 0$ along the crack surfaces. When the lower material is considered rigid, the continuity conditions along the interface become $v_1 = v_2 = 0$, while the tractions there are not restricted.

SOLUTIONS FOR INDIVIDUAL SECTORS

The asymptotic analysis in this section is mainly based on, but in part extended from, previous studies of elastic–plastic crack growth in homogeneous materials by Gao and Nemat-Nasser (1983), Lin (1985), Leighton *et al.* (1987), and Deng and Rosakis (1991), among others. To facilitate such an analysis, it is commonly implicitly assumed that mathematical operations such as $\lim_{r\to 0}(\ )$, $\partial(\ )/\partial r$, $\int(\ )\,dr$, etc., are permitted as needed and that their order of operation can be exchanged and mixed with order symbols $o(\ )$ and $O(\ )$ within each of the possible angular sectors surrounding the crack tip, and final solutions are derived by assembling a spectrum of sectors without violating any underlying mathematical and physical principles. (The small-strain assumption will be violated if strain singularity exists in a solution, which, however, is usually not held against such a solution, in that the singularity represents a spatial characteristic of the physical problem when the crack-tip is approached.) When the elastic–plastic material obeys the maximum plastic work principle, the analysis by Leighton *et al.* (1987) for mode I crack growth in homogeneous materials also holds here, which indicates that the stresses for the interface crack problem must be fully continuous in each of the two component materials, and that the hydrostatic stress σ, hence the stresses, must be bounded, and, as far as a first-order analysis is concerned, can be considered as functions of θ only. In the present study, we are interested in solutions with full velocity-field continuity.

Based on the assumptions listed so far and the consequent field properties discussed above, it can be proved that the velocity field must have the following asymptotic structure at the crack tip, in both elastic and plastic sectors:

$$v_\alpha(r,\theta) = A_\alpha \ln(R/r) + F_\alpha(r) + B_\alpha(\theta) + o(1) \quad \text{as } r \to 0, \tag{6}$$

where A_α are unknown constants; $B_\alpha(\theta)$ are functions of θ only; R is a length scaling parameter; $F_\alpha(r) = o(\ln(R/r))$ but still singular as $r \to 0$; and $o(\ )$ is the infinitesimal order symbol. In the case of mode I crack growth in homogeneous materials, logarithmic velocity singularity must be ruled out (Leighton *et al.*, 1987) if the maximum plastic work principle is invoked, which motivated us also to seek solutions with $A_\alpha = 0$ here, which in fact must hold if the interface is between a ductile material and a rigid substrate. We also note here that the second term in (6) will not enter the equations of the present first-order analysis, and can be omitted for practical purposes (in fact it should disappear if one of the materials is rigid). Therefore, the components of the velocity field, as those of the stress field, will be regarded as functions of θ only, which enables us to construct solutions directly from those in the literature, e.g. that by Leighton *et al.* (1987). To present the elastic–plastic solutions in simple formats, we introduce for plastic sectors a conventional intermediate function $\psi(\theta)$, and express the stress components as

$$\begin{aligned}\sigma_{11}(\theta) &= \sigma(\theta)-k\cos(2\theta-\psi(\theta)),\\ \sigma_{22}(\theta) &= \sigma(\theta)+k\cos(2\theta-\psi(\theta)),\\ \sigma_{12}(\theta) &= -k\sin(2\theta-\psi(\theta)).\end{aligned} \tag{7}$$

It can be verified that when put in the form of eqns (7), stresses automatically satisfy the yield condition (5). Following Leighton *et al.* (1987), among others, it can be shown that there are two possible plastic sectors: one is uniform and the other, nonuniform. In a *uniform plastic sector*, stresses and velocities are all constant, which can be written as

$$\begin{gathered}\psi(\theta)=2\theta+\psi_o,\quad \lambda\equiv 0,\quad \sigma(\theta)\equiv\sigma_o,\quad v_1(\theta)\equiv v_{1o},\quad v_2(\theta)\equiv v_{2o},\\ \sigma_{11}(\theta)\equiv\sigma_0-k\cos\psi_o,\quad \sigma_{22}(\theta)\equiv\sigma_o+k\cos\psi_o,\quad \sigma_{12}(\theta)\equiv k\sin\psi_o,\end{gathered} \tag{8}$$

where quantities with subscript "o" are constants. In a *nonuniform plastic sector*, on the other hand, the solutions are functions of θ, and they are given by

$$\begin{gathered}\cos\psi=(\pm)m\sin\theta,\quad \sin\psi=-(\pm)\sqrt{1-m^2\sin^2\theta},\\ \lambda=(v/2m\mu r)[2\sqrt{1-m^2\sin^2\theta}-m\cos\theta],\\ \sigma(\theta)=\sigma_o-(\pm)k[m\sin\theta-2E(\theta;m)],\\ v_1(\theta)=v_{1o}-(\pm)(kv/m^2\mu)[2m\sin\theta+(1-m^2)F(\theta;m)-E(\theta;m)],\\ v_2(\theta)=v_{2o}-(\pm)(kv/m^2\mu)[-2m\cos\theta+\sqrt{1-m^2\sin^2\theta}],\end{gathered} \tag{9}$$

where the quantities with subscript "o" are generic constants and are in general different from those in eqn (8), and "$\pm$" denotes two possibilities for the value of ψ and so on, both of which lead to positive values for the flow factor λ. (We note here, as well as in later sections, that the use of eqn (7) is implied whenever only $\psi(\theta)$ and $\sigma(\theta)$ are given.) The functions $F(\theta;m)$ and $E(\theta;m)$ are the Legendre elliptic integrals of, respectively, the first and second kind, defined by

$$F(\theta;m)=\int_0^\theta \mathrm{d}\theta/\sqrt{1-m^2\sin^2\theta},\quad E(\theta;m)=\int_0^\theta\sqrt{1-m^2\sin^2\theta}\,\mathrm{d}\theta, \tag{10}$$

where parameter m, often referred to as the Mach number, is related to the material's shear modulus μ and mass density ρ through $m=v/c_s=v/(\mu/\rho)^{1/2}$, c_s being the material's shear wave speed. Finally, in an *elastic sector*, stresses and velocities are again all constant, and, due to full stress continuity (hence the satisfaction of the yield condition), the sector will be equivalent to a uniform plastic one if it is adjacent to a plastic sector in the same component material.

In what follows, a number of one-parameter families of solutions of the asymptotic interfacial crack-tip fields will be presented for ductile/rigid interfaces and several isolated solutions for ductile/ductile interfaces. This is accomplished by assembling a number of elastic–plastic sectors around the crack tip, so as to satisfy the traction-free boundary conditions on the crack surfaces and the traction and velocity continuity conditions along the material interface, as well as such continuity conditions across all inter-sector radial boundaries. Once an assembly of sectors is obtained, the strain distributions in each of the sectors can be derived by integrating the strain-rates, which can be obtained from velocity components through eqn (2), along lines parallel to the x_1-axis, for which x_2 = constant. This is because the strains at a material point are accumulated when the particle is traversing the crack-tip sectors along the negative x_1-direction. After carrying out such integrations, the strains in a nonuniform sector are found to be:

$$\varepsilon_{11} = -\varepsilon_{22} = \varepsilon_{11o} + (\pm)(k/m^2\mu)[2m\sin\theta + (1-m^2)F(\theta;m) - E(\theta;m)],$$

$$\varepsilon_{12} = \varepsilon_{12o} - (\pm)(k/m^2\mu)[2m\cos\theta - \sqrt{1-m^2\sin^2\theta} + m\ln|\tan(\theta/2)| - (m^2/2)\ln|(1-\sqrt{1-m^2\sin^2\theta})/m\sin\theta|], \quad (11)$$

where ε_{11o} and ε_{12o} are, in general, functions of x_2 only. It is also easy to see that strains in a uniform sector are also functions of x_2 only. These functions of x_2 can be considered as constants in a first-order analysis, such as the present one, if singularity in x_2 is ruled out. To this end, it is noted that in a sector bordering the x_1-axis, singularity as $x_2 \to 0$ without regard to the value of x_1, is unreasonable and must be discarded. As such, and upon observing how strains are accumulated, we conclude that ε_{11o}, ε_{12o} and strains in uniform sectors can all be regarded as unknown constants. It is hence concluded that strain fields given by the asymptotic solutions here will not be singular at the crack tip.

DUCTILE/RIGID INTERFACE: TYPE I ASSEMBLY

As shown in Fig. 2, the crack-tip region in the upper ductile material is composed of two uniform plastic sectors, with sector (i) bordering the crack surface and sector (iii) the material interface, and one nonuniform plastic sector, sector (ii), in between. Admissible stress distributions in these sectors belong to four families of solutions, which are given below.

First family

This family of solutions is characterized by a *tensile* normal stress in the x_1-direction along the crack flank. In sector (i) $(\pi \geqslant \theta \geqslant \theta_1)$:

$$\sigma \equiv k, \quad \sigma_{11} \equiv 2k, \quad \sigma_{22} = \sigma_{12} \equiv 0. \quad (12)$$

In sector (ii) $(\theta_1 \geqslant \theta \geqslant \theta_2)$:

$$\cos\psi = -m\sin\theta, \quad \sin\psi = \sqrt{1-m^2\sin^2\theta},$$

$$\sigma = k[m(\sin\theta - \sin\theta_1) - 2E(\theta;m) + 2E(\theta_1;m) + 1]. \quad (13)$$

Finally, in sector (iii) $(\theta_2 \geqslant \theta \geqslant 0)$:

$$\sigma_{11} \equiv \sigma - k\cos\eta, \quad \sigma_{22} \equiv \sigma + k\cos\eta, \quad \sigma_{12} \equiv k\sin\eta, \quad (14)$$

where the mean stress σ is given by the expression in eqn (13) at $\theta = \theta_2$, and η is the arbitrary parameter for this family of solutions, whose range of values is limited by the inequality $\pi > \theta_1 > \theta_2 > 0$ and by the requirement that $\cos\psi < 0$ and $\sin\psi > 0$ at θ_2. The angles θ_1 and θ_2 are determined from the continuity of the tractions across the inter-sector radial boundaries. We then obtain

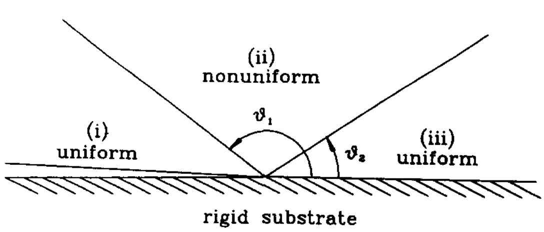

Fig. 2. The type I assembly of plastic sectors around a ductile/rigid interface crack.

$$\theta_1 = \pi - \sin^{-1}[(-m+\sqrt{m^2+8})/4] \tag{15}$$

and we can solve for θ_2 from

$$\cos(2\theta_2+\eta) = -m\sin\theta_2 < 0 \quad \text{and} \quad \sin(2\theta_2+\eta) > 0. \tag{16}$$

For $m = 0.3$, it is found that $\theta_1 = 140.5°$, $-180° < \eta < 90°$, and correspondingly, $140.5° > \theta_2 > 0°$. It can be shown that the stress component σ_{22} for this family of solutions is always tensile in front of the crack tip, whose magnitude increases as η increases. As such, this family of solutions will be referred to as "tensile" solutions. Stress distributions for the cases of $\eta = -60°$ and $60°$ are shown in Figs 3(a) and 3(b), where and thereafter, unless stated otherwise, the stress values are dimensionless due to normalization by the yield stress k.

After the angles are determined from the stress field alone, the velocity and strain fields can be obtained from continuity conditions in a straightforward manner. However, for the sake of brevity, expressions for the velocity and strain components will be given for this particular case only and will be omitted in the sequel. Noting full continuities throughout, we can arrive at the following formulae. In sector (iii), $v_1 = v_2 = \varepsilon_{11} = \varepsilon_{22} = 0$ and $\varepsilon_{12} \equiv \varepsilon_{12o}$, where ε_{12o} is an unknown constant, which cannot be determined asymptotically

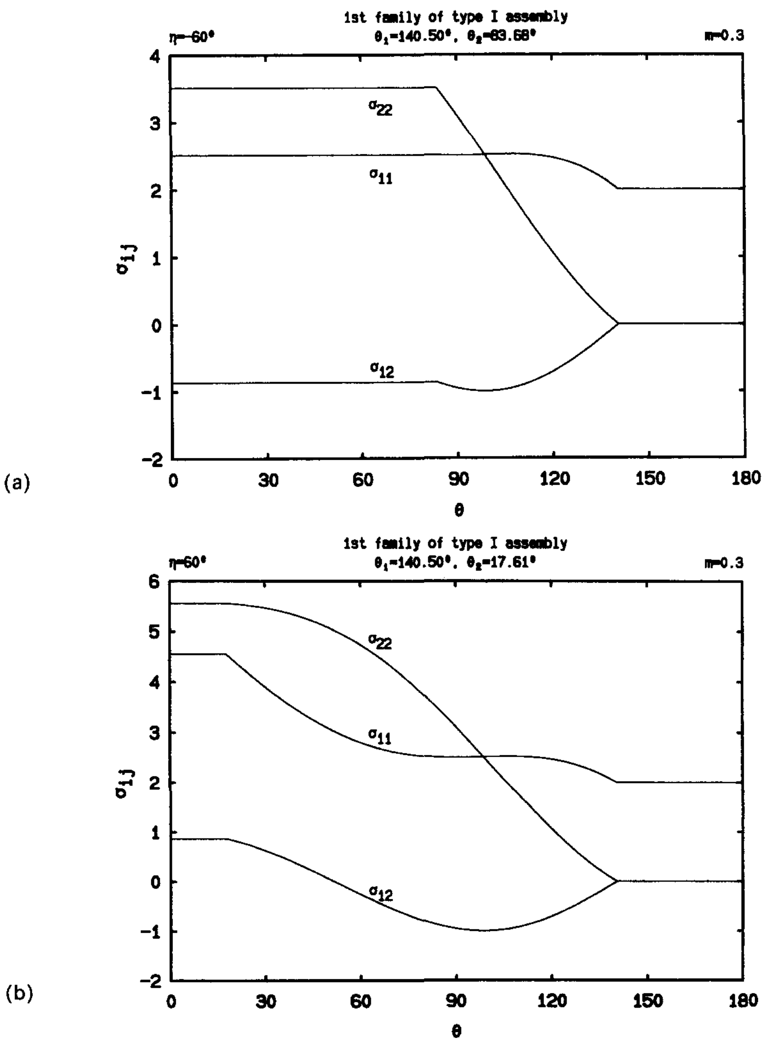

Fig. 3. Angular stress variations for the first family of solutions of type I assembly around a ductile/rigid interface crack, when $m = 0.3$ and (a) $\eta = -60°$ or (b) $\eta = 60°$.

and must be obtained from a full-field analysis, such as a finite element study. The velocities and strains in sector (i) are all constant and their values are equal to those from sector (ii) at $\theta = \theta_1$, which can be written as

$$\begin{aligned} v_1 = v\varepsilon_{22} = -v\varepsilon_{11} = (kv/\mu m^2)[2m(\sin\theta - \sin\theta_2) \\ +(1-m)F(\theta;m) - (1-m)F(\theta_2;m) - E(\theta;m) + E(\theta_2;m)], \\ v_2 = (kv/\mu m^2)[-2m(\cos\theta - \cos\theta_2) + \sqrt{1-m^2\sin^2\theta} - \sqrt{1-m^2\sin^2\theta_2}], \\ \varepsilon_{12} = \varepsilon_{12_0} + (k/\mu m^2)[2m(\cos\theta - \cos\theta_2) - \sqrt{1-m^2\sin^2\theta} \\ + \sqrt{1-m^2\sin^2\theta_2} + m\ln|\tan(\theta/2)/\tan(\theta_2/2)| \\ -(m^2/2)\ln|\sin\theta_2(1-\sqrt{1-m^2\sin^2\theta})/\sin\theta(1-\sqrt{1-m^2\sin^2\theta_2})|]. \end{aligned} \quad (17)$$

Second family

In contrast to the first family, the second family of solutions, also parameterized by η, features a *compressive* normal stress in the x_1-direction along the crack surface. Thus in sector (i), the stresses are:

$$\sigma \equiv -k, \quad \sigma_{11} \equiv -2k, \quad \sigma_{22} = \sigma_{12} \equiv 0. \quad (18)$$

And in sector (iii) the stresses will have the same expressions as those in eqn (14), except that now σ is the mean stress at $\theta = \theta_2$ calculated from the formulae below:

$$\begin{aligned} \cos\psi = m\sin\theta, \quad \sin\psi = -\sqrt{1-m^2\sin^2\theta}, \\ \sigma = -k[m(\sin\theta - \sin\theta_1) - 2E(\theta;m) + 2E(\theta_1;m) + 1], \end{aligned} \quad (19)$$

which is the solution for sector (ii). Finally, it is noted that the angle θ_1 is still given by eqn (15) while θ_2 is determined from:

$$\cos(2\theta_2 + \eta) = m\sin\theta_2 > 0 \quad \text{and} \quad \sin(2\theta_2 + \eta) < 0. \quad (20)$$

The parameter η for this family of solutions is restricted by the requirement that $\cos\psi > 0$ and $\sin\psi < 0$ at θ_2. For $m = 0.3$, we have $\theta_1 = 140.5°$, $-180° < \eta < -90°$ and $0° < \eta < 180°$, and correspondingly, $51.82° > \theta_2 > 0°$ and $140.5° > \theta_2 > 51.82°$. This family of solutions is characterized by a stress state at the crack front of the following type: $\sigma_{22} < 0$ for all η values, and $\sigma_{12} < 0$ for $-180° < \eta < -90°$ and $\sigma_{12} > 0$ for $0° < \eta < 180°$. This seems to imply that if crack growth does occur with this type of stress field, it must be of a shearing type. In light of this, we will label this family of solutions "shear" solutions. The stress distributions for $\eta = -120°$ and $60°$ are given in Figs 4(a) and 4(b).

Third family

Similar to the first family, the crack flank for this family is in a state of uniaxial tension in the x_1-direction. It is noted that stresses in sectors (i) and (iii) will still be described by, respectively, eqns (12) and (14), while those in sector (ii) will be given by a set of formulae slightly different from eqn (19), namely,

$$\begin{aligned} \cos\psi = m\sin\theta, \quad \sin\psi = -\sqrt{1-m^2\sin^2\theta}, \\ \sigma = -k[m(\sin\theta - \sin\theta_1) - 2E(\theta;m) + 2E(\theta_1;m) - 1]. \end{aligned} \quad (21)$$

In this case, the mean stress σ in eqn (14) must be obtained from (21) through continuity at θ_2, which is determined through eqn (20). The angle θ_1 is given by

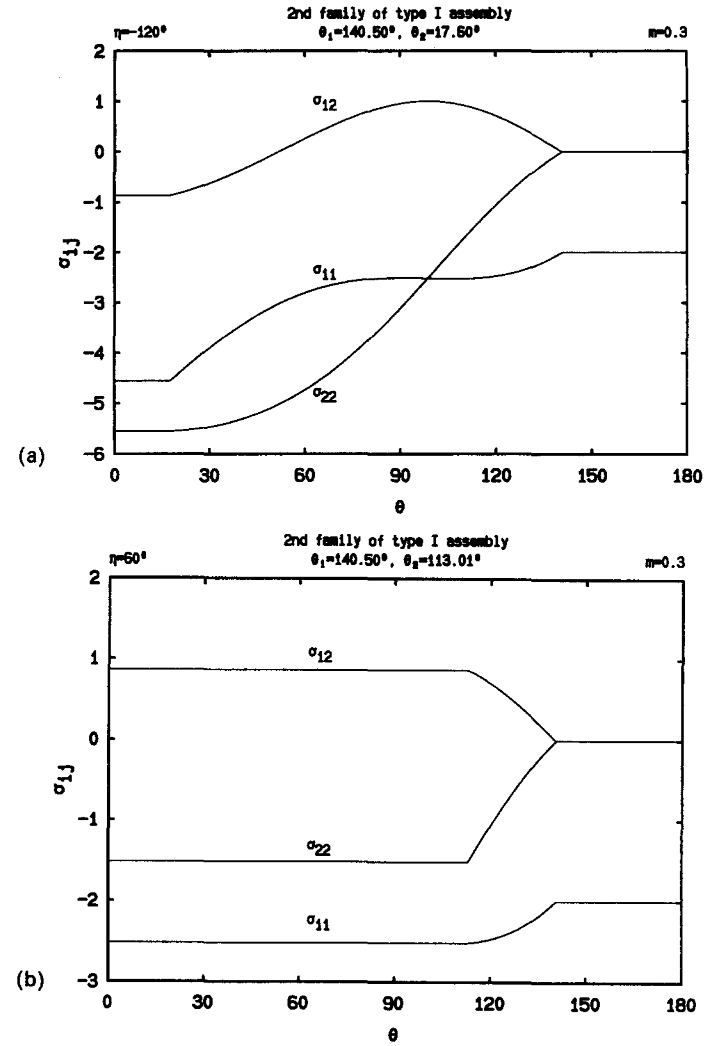

Fig. 4. Angular stress variations for the second family of solutions of type I assembly around a ductile/rigid interface crack, when $m = 0.3$ and (a) $\eta = -120°$ or (b) $\eta = 60°$.

$$\theta_1 = \sin^{-1}[(m+\sqrt{m^2+8})/4]. \tag{22}$$

For $m = 0.3$, $\theta_1 = 51.82°$, $-180° < \eta < -90°$ and correspondingly $51.82° > \theta_2 > 0°$. This family of solutions resembles the previous one, in that at the crack front $\sigma_{22} < 0$ and $\sigma_{12} < 0$ for all η values. Therefore, this family of solutions will also be referred to as "shear" solutions. Figure 5 depicts stress variations for the case of $\eta = -120°$.

Fourth family

Stresses in sectors (i) and (iii) are computed from eqns (18) and (14) respectively, and those in sector (ii) from the following:

$$\cos\psi = -m\sin\theta, \quad \sin\psi = \sqrt{1-m^2\sin^2\theta},$$
$$\sigma = k[m(\sin\theta - \sin\theta_1) - 2E(\theta; m) + 2E(\theta_1; m) - 1]. \tag{23}$$

The angles θ_1 and θ_2 are determined, respectively, from eqns (22) and (16). For $m = 0.3$, $\theta_1 = 51.82°$, $0° < \eta < 90°$ and correspondingly $51.82° > \theta_2 > 0°$. This family of solutions has the same feature as the first family, namely that the stress component σ_{22} at the crack front is always tensile, and hence will also be called "tensile" solutions. The stress variations for the case of $\eta = 60°$ are illustrated in Fig. 6.

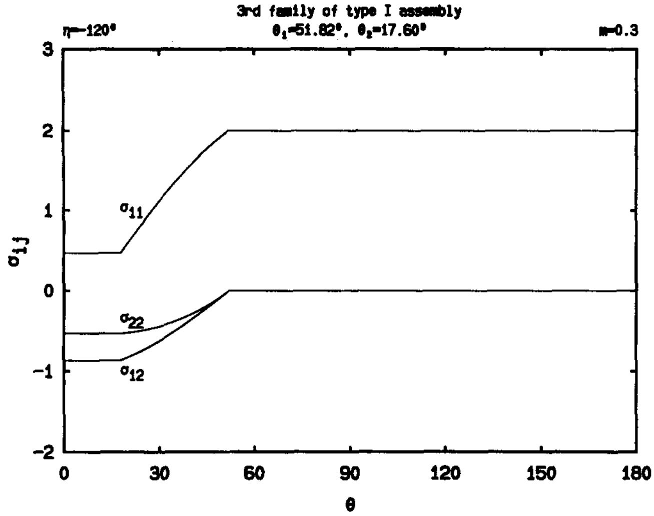

Fig. 5. Angular stress variations for the third family of solutions of type I assembly around a ductile/rigid interface crack, when $m = 0.3$ and $\eta = -120°$.

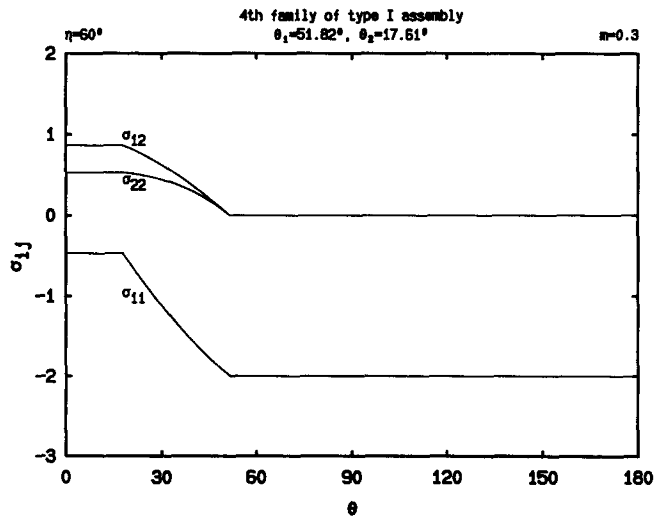

Fig. 6. Angular stress variations for the fourth family of solutions of type I assembly around a ductile/rigid interface crack, when $m = 0.3$ and $\eta = 60°$.

DUCTILE/RIGID INTERFACE: TYPE II ASSEMBLY

The second type of assembly of sectors for the ductile/rigid interface is obtained from the first one by adding a nonuniform plastic sector (iv) between the material interface and the uniform sector (iii), as shown in Fig. 7. Two one-parameter families of solutions exist.

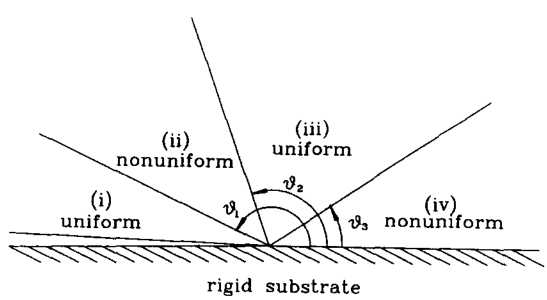

Fig. 7. The type II assembly of plastic sectors around a ductile/rigid interface crack.

First family

The stress distributions in sectors (i)–(iii) and the angles separating the three sectors, namely θ_1 and θ_2, follow the same set of formulae as those for the first family of type I assembly. Stresses in sector (iv) ($\theta_3 \geqslant \theta \geqslant 0$) are obtainable from

$$\cos\psi = m\sin\theta, \quad \sin\psi = -\sqrt{1-m^2\sin^2\theta},$$

$$\sigma = -k[m(\sin\theta-\sin\theta_3-\sin\theta_2+\sin\theta_1)-2E(\theta;m) \\ +2E(\theta_3;m)+2E(\theta_2;m)-2E(\theta_1;m)-1], \quad (24)$$

and the angle θ_3 must be determined from the following conditions:

$$\cos(2\theta_3+\eta) = m\sin\theta_3 > 0 \quad \text{and} \quad \sin(2\theta_3+\eta) < 0, \quad (25)$$

where the parameter η is confined to certain intervals. For $m = 0.3$, $\theta_1 = 140.5°$, $-180° < \eta < -90°$ and correspondingly, $140.5° > \theta_2 > 98.63°$ and $51.82° > \theta_3 > 0°$. This family of solutions is composed of "shear" and "tensile" solutions. For example, for the case $m = 0.3$, it belongs to the group of "shear" solutions (with $\sigma_{12} < 0$ at $\theta = 0°$) when $-180° < \eta < -164°$ and to the group of "tensile" solutions when $-163° < \eta < -90°$. See Fig. 8 for stress variations when $\eta = -120°$.

Second family

Stresses in sectors (i)–(iii) and angles θ_1 and θ_2 are described by the same set of formulae as those for the second family of type I assembly. Stresses in sector (iv) ($\theta_3 \geqslant \theta \geqslant 0$) come from

$$\cos\psi = -m\sin\theta, \quad \sin\psi = \sqrt{1-m^2\sin^2\theta},$$

$$\sigma = k[m(\sin\theta-\sin\theta_3-\sin\theta_2+\sin\theta_1)-2E(\theta;m) \\ +2E(\theta_3;m)+2E(\theta_2;m)-2E(\theta_1;m)-1] \quad (26)$$

and the angle θ_3 is determined from the following conditions:

$$\cos(2\theta_3+\eta) = -m\sin\theta_3 < 0 \quad \text{and} \quad \sin(2\theta_3+\eta) > 0, \quad (27)$$

where η can only vary within a certain range. For $m = 0.3$, $\theta_1 = 140.5°$, $0° < \eta < 90°$ and

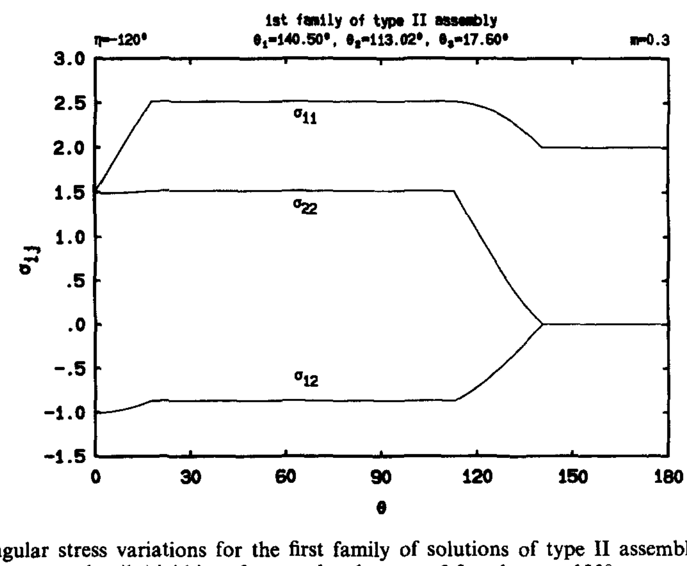

Fig. 8. Angular stress variations for the first family of solutions of type II assembly around a ductile/rigid interface crack, when $m = 0.3$ and $\eta = -120°$.

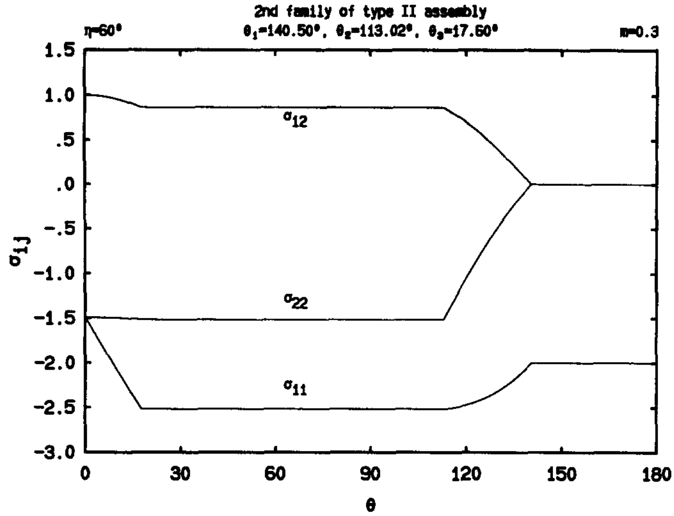

Fig. 9. Angular stress variations for the second family of solutions of type II assembly around a ductile/rigid interface crack, when $m = 0.3$ and $\eta = 60°$.

correspondingly, $140.5° > \theta_2 > 98.63°$ and $51.82° > \theta_3 > 0°$. This family contains mainly "shear" solutions with $\sigma_{12} > 0$ in front of the crack tip. In particular, for $m = 0.3$ the solutions are of the "shear" type when $17° < \eta < 90°$. Stress variations for $\eta = 60°$ are shown in Fig. 9.

DUCTILE/DUCTILE INTERFACE: ISOLATED SOLUTIONS

Interfaces in many composite materials are between a ductile material and a brittle material and are often modelled as ductile/rigid interfaces, as done in most previous studies as well as in the earlier sections of this paper. The results of the finite element study by Shih and Asaro (1989) indicate that for a ductile/ductile interface, the asymptotic behavior of the stress field at the crack tip is governed by the softer (more ductile) material, implying that asymptotic solutions for a ductile/rigid interface can capture the essential features of the crack-tip fields in the more ductile material for a ductile/ductile interface. On the other hand, while analytical solutions for ductile/ductile interfaces are expected to provide more accurate descriptions of the interfacial crack-tip fields and hence more desirable, they are mathematically much more involved and hence more difficult to obtain. Nonetheless, since asymptotic analyses usually involve many simplifying assumptions, the existence of asymptotic solutions under these assumptions for ductile/ductile interfaces will have theoretical significance. In the following we demonstrate the existence of two types of such solutions for a pair of dissimilar ductile materials. These two types of solutions are referred to as "isolated solutions" here since they do not represent families of solutions with free parameters. They share the same assembly of plastic sectors around the crack tip, which as shown in Fig. 10 is composed of two uniform sectors and one nonuniform sector in each

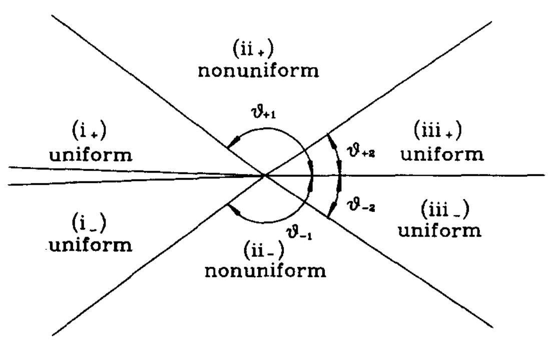

Fig. 10. An assembly of plastic sectors around a ductile/ductile interface crack.

of the ductile materials. As a convention, subscripts "+" and "−" will be used to signify quantities (such as the yield stress k, the Mach number m, the angles separating the different sectors, and the parameter η) associated with, respectively, the upper and lower materials. Stress variations for both solutions are given below.

First solution

For the upper material, the solution is represented by that for the first family of solutions of the type I crack-tip assembly for a ductile/rigid interface, with relevant quantities indicated by a subscript "+". For the lower material, the solution is given by, for sector (i_-):

$$\sigma = k_-, \quad \sigma_{11} = 2k_-, \quad \sigma_{22} = \sigma_{12} = 0; \tag{28}$$

for sector (ii_-):

$$\cos\psi = m_- \sin\theta, \quad \sin\psi = -\sqrt{1-m_-^2\sin^2\theta},$$
$$\sigma = -k_-[m_-(\sin\theta-\sin\theta_{-1})-2E(\theta;m_-)+2E(\theta_{-1};m_-)-1]; \tag{29}$$

and for sector (iii_-):

$$\sigma_{11} \equiv \sigma_- - k_-\cos\eta_-, \quad \sigma_{22} \equiv \sigma_- + k_-\cos\eta_-, \quad \sigma_{12} \equiv k_-\sin\eta_-, \tag{30}$$

where $\sigma_- = \sigma(\theta_{-2})$ from eqn (29). The angle θ_{-1} is computed from

$$\theta_{-1} = -\pi + \sin^{-1}[(-m_- + \sqrt{m_-^2+8})/4] \tag{31}$$

and the angle θ_{-2} should be obtained from

$$\cos(2\theta_{-2}+\eta_-) = m_-\sin\theta_{-2} < 0 \quad \text{and} \quad \sin(2\theta_{-2}+\eta_-) < 0. \tag{32}$$

It must be pointed out that the parameters η_+ and η_- are not arbitrary and must be determined by satisfying the traction continuity conditions across the bimaterial interface at $\theta = 0°$, namely,

$$\sigma_+ + k_+\cos\eta_+ = \sigma_- + k_-\cos\eta_-,$$
$$k_+\sin\eta_+ = k_-\sin\eta_-, \tag{33}$$

where σ_+ and σ_- are the mean stresses in sectors (iii_+) and (iii_-) respectively and are dependent indirectly on η_+ and η_- respectively. It is noted that for a certain crack propagation speed v, the Mach numbers m_+ and m_- for the upper and lower materials will be different due to different shear wave speeds in the two materials. To obtain a solution from eqn (33), the crack speed and the ratios between m_+ and m_-, and between k_+ and k_- must be supplied as input. For example, for the case of $m_+ = 0.4$, $m_- = 0.3$, $k_+ = 1.0$ and $k_- = 1.2$, it is found that $\eta_+ = 33.96°$ and $\eta_- = 27.75°$, and the resulting stress variations

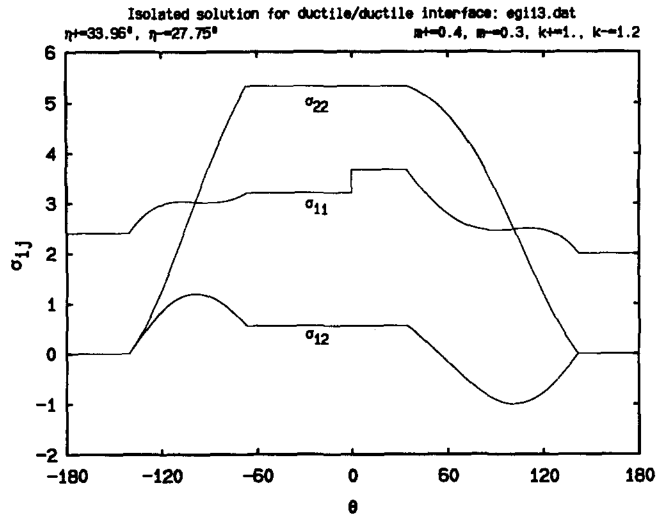

Fig. 11. The first type of isolated solutions for a ductile/ductile interface crack for the case of $m_+ = 0.4, m_- = 0.3, k_+ = 1.0, k_- = 1.2$.

are shown in Fig. 11, where a jump in σ_{11} across the material interface at $\theta = 0°$ is observed. It can be seen that this is a "tensile" solution.

Second solution

For the upper material, the solution is represented by that for the second family of solutions of the type I crack-tip assembly for a ductile/rigid interface, with relevant quantities indicated by a subscript "+". For the lower material, the solution is given by, for sector (i$_-$):

$$\sigma = -k_-, \quad \sigma_{11} = -2k_-, \quad \sigma_{22} = \sigma_{12} = 0; \tag{34}$$

and for sector (ii$_-$):

$$\cos\psi = -m_- \sin\theta, \quad \sin\psi = \sqrt{1-m_-^2 \sin^2\theta},$$
$$\sigma = k_-[m_-(\sin\theta - \sin\theta_{-1}) - 2E(\theta; m_-) + 2E(\theta_{-1}; m_-) - 1]. \tag{35}$$

Stresses for sector (iii$_-$) are still described by eqn (30), except that $\sigma_- = \sigma(\theta_{-2})$ should be calculated from eqn (35). The angle θ_{-1} is the same as that given by eqn (31), but θ_{-2} should come from

$$\cos(2\theta_{-2} + \eta_-) = -m_- \sin\theta_{-2} > 0 \quad \text{and} \quad \sin(2\theta_{-2} + \eta_-) > 0. \tag{36}$$

Again, the parameters η_+ and η_- are not arbitrary and must be determined from the traction continuity conditions in eqn (33). For the case of $m_+ = 0.4$, $m_- = 0.3$, $k_+ = 1.0$ and $k_- = 1.2$, it is found that $\eta_+ = -146.03°$ and $\eta_- = -152.25°$. The stress distributions are shown in Fig. 12. This is a "shear" solution with $\sigma_{12} < 0$ at $\theta = 0°$.

CLOSING COMMENTS

A first-order elastic–plastic asymptotic analysis has been carried out for the problem of plane strain, steady-state dynamic crack growth along ductile/rigid and ductile/ductile interfaces. The ductile materials are elastic–perfectly plastic and incompressible, and obey the J_2-flow theory of plasticity. Six one-parameter families of solutions are found for ductile/rigid interfaces and two types of isolated solutions for ductile/ductile interfaces. The velocity and strain fields for these solutions are not singular at the crack tip, and full velocity

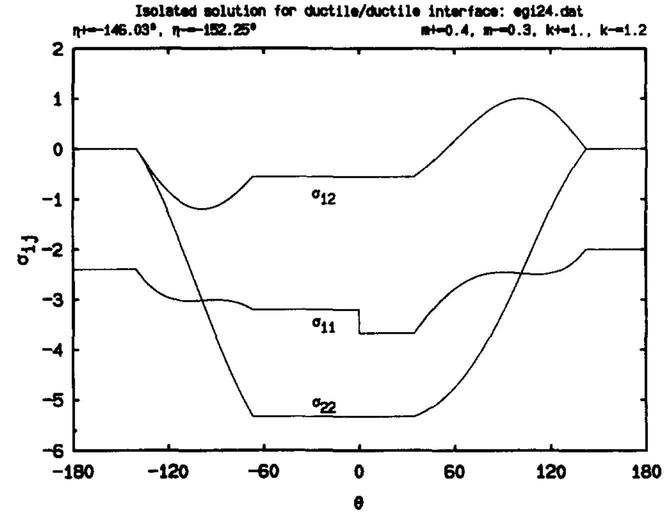

Fig. 12. The second type of isolated solutions for a ductile/ductile interface crack for the case of $m_+ = 0.4, m_- = 0.3, k_+ = 1.0, k_- = 1.2$.

and stress continuities are achieved in each of the two component materials. The following observations can be made about the above study:

(a) The solutions reported here represent a class of possible mathematical structures of the near-tip fields for dynamically growing interfacial cracks. Whether they can be achieved in reality or not must be examined against full-field solutions for properly posed boundary/initial value problems obtained with, for example, the finite element methods. Such full-field numerical solutions are not yet available.

(b) While two types of isolated solutions are demonstrated in this study for ductile/ductile interfaces, families of solutions with free parameters are not attempted (although it is suspected that several assemblies of crack-tip plastic sectors are possible based on our understanding of the asymptotic structures in each of the plastic sectors). This is because, as mentioned earlier, the study by Shih and Asaro (1989) indicates that for a ductile/ductile interface, the asymptotic behavior of the stress field at the crack tip is governed by the softer (more ductile) material, implying that asymptotic solutions for a ductile/rigid interface can capture the essential features of the crack-tip fields in the more ductile material for a ductile/ductile interface. As such, it makes more sense that such possibilities be explored if full-field numerical studies are available and if they suggest the existence of such families of solutions.

(c) The various types of solutions given in this paper have been roughly labelled as "tensile" or "shear" solutions. Some of the "tensile" solutions do not have significant tensile σ_{22} values in front of the crack tip and if crack growth can occur in this case the driving force must be from the shear stress component σ_{12}. In this connection, it is noted that the "shear" solutions sometimes have positive σ_{12} values and sometimes negative values at $\theta = 0°$, which may not all be possible for traction-free interface cracks, because if they correspond to, respectively, remote positive and negative shear loading, then under certain conditions one of them will cause crack surface contact over a length scale larger than the plastic zone size. For example, for the geometry of the ductile/rigid interface cracks considered, a negative remote shear loading will cause non-negligible crack surface contact for a crack along the interface of a compressible linearly elastic solid and a rigid substrate, and asymptotic solutions assuming, say, frictionless crack surface contact must be obtained along the line of this study.

Acknowledgements—This work was supported in part by a research start-up grant from the College of Engineering of the University of South Carolina, Columbia, SC, and by a grant from the University of South Carolina Research and Productive Scholarship Fund.

REFERENCES

Aravas, N. and Sharma, S. M. (1991). An elastoplastic analysis of the interface crack with contact zones. *J. Mech. Phys. Solids* **39,** 311–344.

Champion, C. R. and Atkinson, C. (1990). A mode III crack at the interface between two nonlinear materials. *Proc. Roy. Soc. Lond. A* **429,** 247–257.

Champion, C. R. and Atkinson, C. (1991). A crack at the interface between two power-law materials under plane strain loading. *Proc. Roy. Soc. Lond. A* **432,** 547–553.

Deng, X. and Rosakis, A. J. (1991). Dynamic crack propagation in elastic–perfectly plastic solids under plane stress conditions. *J. Mech. Phys. Solids* **39,** 683–722.

Deng, X. (1992). Plane strain near-tip fields for elastic–plastic interface cracks. MECH Report 92-2, Department of Mechanical Engineering, University of South Carolina, Columbia, SC 29208, USA.

Drugan, W. J. (1991). Near-tip fields for quasi-static crack growth along a ductile-brittle interface. *J. Appl. Mech.* **58,** 111–119.

Gao, Y. and Lou, Z. (1990). Mixed mode interface crack in a pure power-hardening bimaterial. *Int. J. Fract.* **43,** 241–256.

Gao, Y. C. and Nemat-Nasser, S. (1983). Dynamic fields near a crack tip in an elastic–perfectly-plastic solid. *Mech. Mater.* **2,** 47–60.

Guo, Q. and Keer, L. M. (1990a). A crack at the interface of two power-law hardening materials—Antiplane case. *J. Mech. Phys. Solids* **38,** 183–194.

Guo, Q. and Keer, L. M. (1990b). A crack at the interface between an elastic–perfectly plastic solid and a rigid substrate. *J. Mech. Phys. Solids* **38,** 843–857.

Leighton, J. T., Champion, C. R. and Freund, L. B. (1987). Asymptotic analysis of steady dynamic crack growth in an elastic–plastic material. *J. Mech. Phys. Solids* **35,** 541–563.

Lin, B. (1985). Elastic perfectly-plastic fields at a rapidly propagating crack-tip. *Appl. Math. Mech.* **6,** 1017–1025.

Ponte Castaneda, P. and Mataga, P. A. (1991). Stable crack growth along a brittle/ductile interface—I. Near-tip fields. *Int. J. Solids Structures* **22,** 105–133.

Sharma, S. M. and Aravas, N. (1991). Plane stress elastoplastic solutions of interface cracks with contact zones. *Mech. Mater.* **12,** 147–163.

Shih, C. F. and Asaro, R. J. (1988). Elastic–plastic analysis of cracks on bimaterial interfaces: Part I—Small scale yielding. *J. Appl. Mech.* **55,** 299–316.

Shih, C. F. and Asaro, R. J. (1989). Elastic–plastic analysis of cracks on bimaterial interfaces: Part II—Structure of small-scale yielding fields. *J. Appl. Mech.* **56,** 763–779.

Wang, T. C. (1990). Elastic–plastic asymptotic fields for cracks on bimaterial interfaces. *Engng Fract. Mech.* **37,** 527–538.

Zywicz, E. and Parks, D. M. (1990). Elastic–plastic analysis of frictionless contact at interfacial crack tips. *Int. J. Fract.* **42,** 129–143.

Zywicz, E. and Parks, D. M. (1992). On small-scale yielding interfacial crack-tip fields. *J. Mech. Phys. Solids* **40,** 511–536.